Simultaneous enhancement of toughness, ductility, and strength of nanocrystalline ceramics at high strain-rates

Yifei Mo and Izabela Szlufarska[a)]
Department of Materials Science and Engineering, University of Wisconsin, Madison, Wisconsin 53706

(Received 21 March 2007; accepted 12 April 2007; published online 4 May 2007)

Molecular dynamics simulations of tensile testing have been performed on nc-SiC. Reduction of grain size promotes simultaneous enhancement of ductility, toughness, and strength. nc-SiC fails by intergranular fracture preceded by atomic level necking. Conventionally, high strain-rate deformations of ceramics are limited by diffusion time scales, since diffusion prevents premature cavitation and failure. The authors report a nondiffusional mechanism for suppressing premature cavitation, which is based on unconstrained plastic flow at grain boundaries. Based on the composite's rule of mixture, they estimate Young's modulus of random high-angle grain boundaries in nc-SiC to be about 130 GPa. © *2007 American Institute of Physics*. [DOI: 10.1063/1.2736652]

One of the main limitations in the applications of ceramics is their lack of ductility, which inhibits the ability to form and manufacture these strong and hard materials.[1,2] Preventing mechanical failure in ceramic-based engineering components is particularly challenging during tensile deformations because a tensile stress causes opening of preexisting cracks, leading to failure by fast brittle fracture. A number of studies have been reported on the effect of preexisting flaws on strength and toughness of ceramics.[3–5] In general, the maximum true stress reached in these materials corresponds to fracture strength, which is governed by largest-flaw statistics. As a result, experimental values of strength show a large degree of variability and it has not yet been established whether nanoceramics will exhibit improved fracture toughness.[6,7] In recent years, there have been significant experimental efforts to synthesize fine-grained ceramics that would be free of preexisting flaws, e.g., cracks or pores.[7,8] However, a tensile deformation of these materials will still be limited by premature intergranular fracture caused by cavitation at grain boundaries (GBs). Cavities can develop wherever deformation becomes localized, e.g., at the GB junctions during GB sliding.[9] In order to suppress cavitation, the accumulated local stress needs to be relaxed by diffusion processes along GBs,[10–12] and the diffusion time scales set an upper limit on the deformation strain rate. Because high strain-rate deformations are of technological interest for the shape forming of ceramics, the ability to prevent premature failure at high strain rates will have a large impact on the manufacturing processes. Recently, a synthesis of high strain-rate (up to 1 s^{-1}) superplastic ceramics composites has been reported,[2] where an additional stress relaxation was accomplished by dislocation-induced plasticity in the grains (of average diameter of 210 Å). The main challenge in achieving strain rates significantly higher than 1 s^{-1} is to find a method to suppress cavitation when the conventional relaxation mechanisms (e.g., diffusion) are inhibited by the shortened time scales. Computer simulations based on molecular dynamics (MD) are perfectly suited to explore high strain-rate limits of deformation and to unravel its atomistic details.[13] We have performed MD simulations of tensile deformation of nanocrystalline (nc) silicon carbide (SiC) at a strain rate of 10^8 s^{-1}. Our study reveals suppressed cavitation in the absence of diffusion and in the absence of significant dislocation activity in the grains. The suppressed cavitation is primarily due to the reduction of the grain size and is governed by plastic flow along GBs, which delays localization of deformation. We show that the nc-SiC exhibits increased ductility and toughness without compromising its strength. This behavior is quite surprising given that both Young's modulus and yield stress decrease with the decreasing grain size. These excellent mechanical properties complement previously discovered superhardness of nc-SiC,[14,15] as well as other demonstrated or expected superior properties of nc ceramics.[6,16–18] Optimization of mechanical properties through decreasing the grain diameter to the nanometer length scales has been already reported for nc metals.[19] However, the unique mechanical properties of nc metals are primarily governed by the crossover from the intra- to intergranular dislocation activity, while the simultaneous enhancement of strength and toughness of nc ceramics, as reported here, is dominated by suppressed cavity nucleation in a confined intergranular film.

We have prepared a number of computer-generated nc-SiC samples with grain diameter d between 3 and 20 nm. Each sample consists of 32 grains with random high-angle GBs and the largest sample is comprised of $\sim 18\times 10^6$ atoms. All samples have been prepared with the same random grain orientations and the same distribution of grain centers (scaled to give the desired d). A high-pressure high-temperature sintering schedule has been chosen for each sample in such a way so to generate GBs of $\sim$1 nm thickness, which is consistent with experiments.[5,20] The interatomic potential utilized here for SiC is the same as used in our previous studies.[15,21]

nc-SiC is a two-phase material consisting of crystalline grains and highly disordered GBs.[15,22] A sample with $d=16$ nm is shown in Fig. 1(a), where selection of GB atoms is based on a medium-range topological order determined through shortest-path ring statistics.[23] Using this criterion, we determine a volume fraction V_{GB} of GBs and of the crystalline phase $V_{cr}=1-V_{GB}$. Figure 1(b) shows Young's modulus E_{nc} of the nc-SiC samples as a function of V_{GB} as extracted from the tensile tests. Our simulations show that E_{nc} decreases with increasing V_{GB} (decreasing d). Treating nc-

[a)]Electronic mail: izabela@engr.wisc.edu

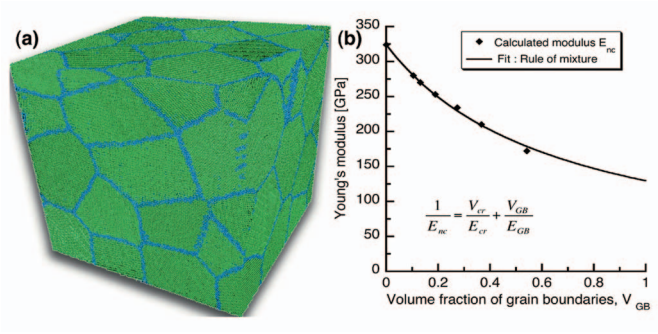

FIG. 1. (Color) (a) Computer-generated sample of nc-SiC with $d=16$ nm. Green color represents ordered crystalline 3*C*-SiC lattice and blue—a disordered GB structure. (b) Young's moduli of nc-SiC as a function of the GB volume fraction V_{GB}. Fitting (solid line) to the Reuss rule of mixture (equation on the plot) yields GB modulus of 130 GPa (±2.5%).

SiC as a composite, we use Reuss rule of mixture to estimate effective modulus E_{GB} of GBs for each sample and we find a consistent value of 130 GPa (±2.5%). The excellent agreement among all samples demonstrates a high level of accuracy of the ring-statistics technique in identifying GB atoms as well as the effectiveness of the presented simulation schedule in extracting elastic moduli of GBs.

All of the samples have been subjected to a simulated tensile testing, in which the simulation box is expanded in the vertical direction while it is allowed to relax in the horizontal directions to account for the Poisson effect. The true stress σ vs true strain ε curves are plotted in Fig. 2(a) and they reveal a reduction of yield stress with decreasing grain diameter d. It can be expected that reduced yield stress will yield to increased ductility and tensile toughness. Ductility is

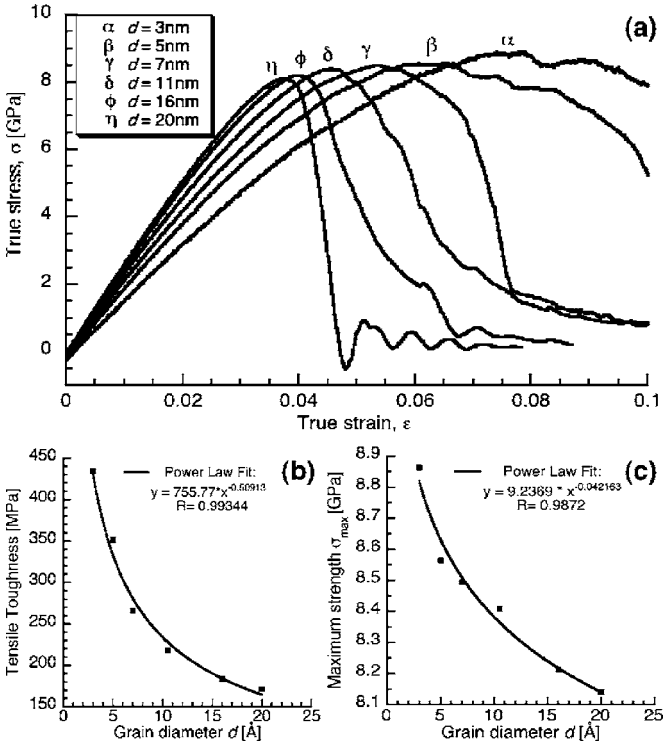

FIG. 2. (a) Stress (σ) vs strain (ε) curves for samples with varying grain size. (b) Tensile toughness calculated as the area under the σ-ε curves up to the point of maximum strength σ_{max} shows increasing toughness with decreasing grain size. (c) σ_{max} plotted as a function of d shows a tendency to strengthen the material with the grain size reduction.

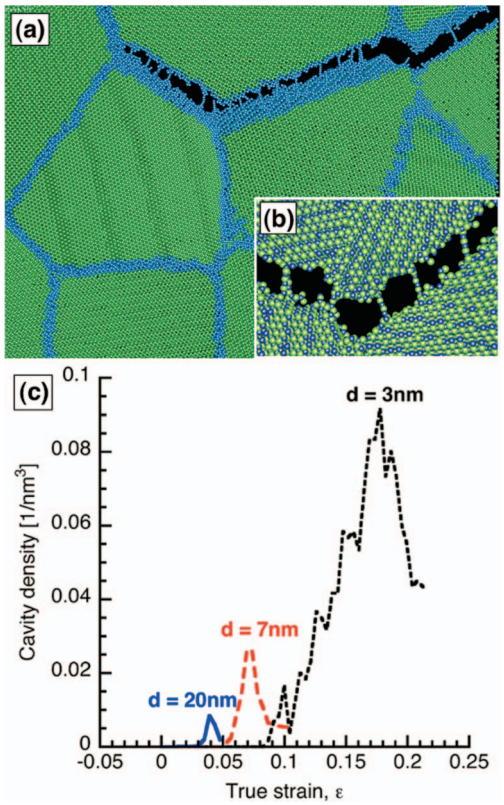

FIG. 3. (Color) (a) Intercrystalline fracture of the $d=16$ nm sample along GBs normal to the direction of applied strain. Color-coding consistent with that in Fig. 1(a). (b) Atomic-level necking leads to formation of one-atom thick chains of alternating Si (blue) and C (green) atoms. (c) Cavity density as a function of strain shows suppressed cavitation in samples with smaller grain sizes.

a measure of how much strain can be applied before a mechanical failure occurs. Here, we define ductility as the strain ε_{max} at the point of maximum stress σ_{max} and as expected, it is larger for samples with smaller d. Tensile toughness is the energy density transferred to a deformed sample and it can be calculated as the total area under the σ-ε curve up to the point of failure (here up to ε_{max}). As shown in Fig. 2(b), tensile toughness increases by about 140% when the grain size is reduced from 20 to 3 nm. Reduced Young's modulus and reduced yield stress are often correlated with a reduced maximum strength σ_{max}. However, the opposite is true for the curves shown in Fig. 2(a). Reduction of the grain size to 3 nm is correlated with a slight (8.5%) increase in σ_{max} as compared to the $d=20$ nm sample [Fig. 2(c)]. To test the reproducibility, these simulations have been repeated for selected grain sizes on samples prepared with a slightly altered sintering schedule. The resulting spread in σ_{max} is about 0.1%.

The unexpected simultaneous enhancement of the ductility, tensile toughness, and σ_{max} can be understood in light of the failure mechanism. As visualized in Fig. 3(a), the primary mechanism of failure is intergranular fracture. In all samples, ε_{max} corresponds to the initial nucleation of oval cavities along the GB normal to the direction of the applied strain, without localization at the GB junctions. The material between the cavities can be thought of as small tensile specimens that are subject to necking at the nanoscale. Before the final fracture, the nanoscale necks are drawn out to form one-atom thick (monatomic) chains of alternating Si and C atoms [Fig. 3(b)]. These chains can be as long as 11 atoms

and they are metastable, i.e., they remain stable during a separate equilibration simulation, in which the strain is kept constant and the stresses are allowed to relax. The observed trend in σ_{max} can be explained by the mechanism of suppressed cavity nucleation. A disordered intergranular film in nc-SiC is quite ductile; however, its plastic flow is constrained by the surrounding rigid grains. As a result, large triaxial stresses develop at GBs during tensile loading, which at a critical stress causes cavitation instabilities. At lower strain rates, cavity nucleation can be suppressed by increased atomic diffusion along GBs; however, the diffusional mechanism is not active in the high-strain limit explored in our simulations. Instead, stress relaxation is accomplished by plastic flow along GBs. Since smaller grains provide less constraint, stress relaxation becomes more efficient in those samples, thus deferring deformation localization that precedes final failure. A suppressed cavitation due to the grain size reduction is illustrated in Fig. 3(c), which shows the cavity density in the $d=3$, 7, and 20 nm samples. A cavity is defined here as a cluster of three or more voids ($4\times4\times4$ Å^3 each). Nucleation of cavities begins at $\varepsilon=\varepsilon_{max}$, and this is the limit we use to define ductility and toughness. However, the final fracture does not take place until the cavities percolate through the system and this event correspond to the maximum in the cavity density plotted in Fig. 3(c). For samples with larger grains size, e.g., $d=20$ nm, the onset of nucleation (at ε_{max}) and the final fracture occur at comparable strains; however, in samples with smaller grains, e.g., $d=3$ nm, the final fracture takes place at strains approximately twice the value of ε_{max}. If the final fracture strain, corresponding to cavity percolation, were used to calculate ductility and toughness in Figs. 2(b) and 2(c), the grain size effects would be even more pronounced.

We have not found any lattice instabilities[24] or any new dislocations nucleated in the grains during the tensile deformation. Plasticity was primarily mediated by deformations in amorphouslike GBs.

The ability to control atomistic mechanisms underlying premature mechanical failure of ceramics during tensile testing, particularly at high strain rates, could have a large impact on engineering design at length scales spanning from nano- to macroscale. Examples include nanoelectromechanical devices, bone implants, hard coatings resistant to harsh environments, and structural engineering components. We have explored the limit of high strain rates, where the main stress relaxation mechanism is intergranular plastic flow. We found that reducing the grains size of nc-SiC leads to superior fracture toughness, ductility, and strength. For a reliable design of ceramics with desired mechanical properties, a complete map of time- and length-scale dependences of all relaxation mechanisms is needed.

Our simulations also suggest a method by which monatomic chains of SiC could be synthesized. While SiC nanowires have been fabricated in the last decade and considered as building block for miniaturization of electronic devices, monatomic SiC nanowires have not been proposed yet. Such nanostructures could exhibit novel chemical and electronic properties as it has been demonstrated for gold nanowires.[25,26] Because SiC is a wide band-gap semiconductor, it is possible that electronic properties of monatomic SiC nanowires in altered chemical environments will be important for device physics.

The authors thank A. Nakano for his code to calculate cavity percolation. They gratefully acknowledge financial support from NSF (DMR-0512228).

[1] N. P. Padture, J. Am. Ceram. Soc. **77**, 519 (1994).
[2] B.-N. Kim, K. Hiraga, K. Morita, and Y. Sakka, Nature (London) **431**, 288 (2002).
[3] M. Ippolito, A. Mattoni, L. Colombo, and F. Cleri, Appl. Phys. Lett. **87**, 141913 (2005).
[4] R. O. Ritchie, Int. J. Fract. **100**, 55 (1999).
[5] D. Chen, M. E. Sixta, X. F. Zhang, L. C. D. Johnghe, and R. O. Ritchie, Acta Mater. **48**, 4599 (2000).
[6] X. T. Wang, N. P. Padture, H. Tanaka, and A. L. Ortiz, Acta Mater. **53**, 271 (2005).
[7] Y. Zhao, J. Qian, L. L. Daemen, C. Pantea, J. Zhang, G. A. Voronin, and T. W. Zerda, Appl. Phys. Lett. **84**, 1356 (2004).
[8] E. A. Ekimov, A. G. Gavriliuk, B. Palosz, S. Gierlotka, P. Dluzewski, E. Tatianin, Y. Kluev, A. M. Naletov, and A. Presz, Appl. Phys. Lett. **77**, 954 (2000).
[9] W. E. Luecke, S. M. Wiederhorn, B. J. Hockey, R. F. Krause, and G. G. Long, J. Am. Ceram. Soc. **78**, 2085 (1995).
[10] A. G. Evans, J. R. Rice, and J. P. Hirth, J. Am. Ceram. Soc. **63**, 368 (1980).
[11] I. A. Ovid'ko, Rev. Adv. Mater. Sci. **10**, 89 (2005).
[12] B. F. Dyson, Met. Sci. **10**, 349 (1976).
[13] D. Wolf, V. Yamakov, S. R. Phillpot, A. Mukherjee, and H. Gleiter, Acta Mater. **53**, 1 (2005).
[14] F. Liao, S. L. Girshick, W. M. Mook, W. W. Gerberich, and M. R. Zachariah, Appl. Phys. Lett. **86**, 171913 (2005).
[15] I. Szlufarska, A. Nakano, and P. Vashishta, Science **309**, 911 (2005).
[16] H. Gleiter, Acta Mater. **48**, 1 (2000).
[17] J. Li and S. Yip, Comput. Model. Eng. Sci. **3**, 219 (2002).
[18] R. W. Siegel, in *Nanomaterials: Synthesis, Properties and Applications*, edited by A. S. Edelstein and R. C. Cammarata (Institute of Physics IOP, Bristol, England, 1996), pp. 201–218.
[19] J. Schiotz and K. W. Jacobsen, Science **301**, 1357 (2003).
[20] J. Wan, R.-G. Duan, M. J. Gash, and A. Mukherjee, Acta Mater. **89**, 274 (2006).
[21] I. Szlufarska, R. K. Kalia, A. Nakano, and P. Vashishta, Appl. Phys. Lett. **86**, 021915 (2005).
[22] P. Keblinski, S. R. Phillpot, D. Wolf, and H. Gleiter, Phys. Rev. Lett. **77**, 2965 (1996).
[23] I. Szlufarska, R. K. Kalia, A. Nakano, and P. Vashishta, Phys. Rev. B **71**, 174113 (2005).
[24] M. Tang and S. Yip, J. Appl. Phys. **76**, 2719 (1994).
[25] H. Hakkinen, R. N. Barnett, and U. Landman, J. Phys. Chem. B **103**, 8814 (1999).
[26] P. Jelinek, R. Perez, J. Ortega, and F. Flores, Phys. Rev. Lett. **96**, 046803 (2006).